On the rate coefficient of the $N(^2D)+O_2\rightarrow NO+O$ reaction in the terrestrial thermosphere

J. W. Duff and H. Dothe

Spectral Sciences, Inc., Burlington, Massachusetts, USA

R. D. Sharma

Space Vehicles Directorate/VSSSE, Air Force Research Laboratory, Hanscom AFB, Massachusetts, USA

[1] The temperature dependence of the rate coefficient of the $N(^2D)+O_2\rightarrow NO+O$ reaction has been determined using *ab initio* potential energy surfaces (PES) and classical dynamics. The calculation agrees with the recommended rate coefficient at 300 K (~110 km altitude). The rate coefficient is given by the expression $k(T) = 6.2 \times 10^{-12}(T/300)$ cm^3/s/molec. In contrast to the nearly temperature-independent value of this rate coefficient previously recommended, the value given here increases by almost a factor of about four as the altitude increases from 110 to 200 km. It is also shown that even though $N(^2D)$ atoms in the thermosphere are produced with large translational energies, using the value of the rate coefficient at the local temperature introduces negligible error in the amount of NO produced. The new value of this rate coefficient will significantly increase the amount of NO computed in the aeronomic models causing a re-evaluation of the heat budget and temperature and density structure of the thermosphere. In particular, implications of the larger rate coefficient for the recent observations of dramatically enhanced 5.3 μm emission from NO in the thermosphere due to solar storms are discussed. *INDEX TERMS:* 0355 Atmospheric Composition and Structure: Thermosphere—composition and chemistry; 0358 Atmospheric Composition and Structure: Thermosphere—energy deposition. **Citation:** Duff, J. W., H. Dothe, and R. D. Sharma, On the rate coefficient of the $N(^2D)+O_2\rightarrow NO+O$ reaction in the terrestrial thermosphere, *Geophys. Res. Lett.*, *30*(5), 1259, doi:10.1029/2002GL016720, 2003.

1. Introduction

[2] Nitric oxide is formed in the terrestrial thermosphere during the day by the reaction of N atoms, mostly ground state $N(^4S)$ and metastable excited state $N(^2D)$, with O_2 [*Barth*, 1992; *Sharma et al.*, 1998]. The dominant mechanism for producing NO in the daylit lower thermosphere where most of the NO is produced is the reaction involving the metastable $N(^2D)$ atoms [*Sharma et al.*, 1998; *Barth et al.*, 1999]. In the upper thermosphere, however, where the temperature is high enough for atom-molecule pairs to have center-of-mass energy in excess of the 0.3 eV activation energy needed for the reaction to proceed, the reaction of ground state $N(^4S)$ atoms with O_2 dominates in the pro-

duction of NO [*Sharma et al.*, 1998]. Copious amounts of NO are also produced at high latitudes in the terrestrial thermosphere during nocturnal auroral precipitation, the dominant mechanism in the lower, as well as the upper thermosphere, being the reaction of metastable $N(^2D)$ atoms with O_2 [*Solomon et al.*, 1999; *Sharma et al.*, 2001; *Dothe et al.*, 2002a]. Because of its importance in the chemistry, energy budget, and dynamics of the terrestrial atmosphere, NO has been the subject of intensive investigations [*Siskind et al.*, 1997; *Sharma and Roble*, 2001]. The room temperature rate coefficient of the reaction of metastable $N(^2D)$ atoms with O_2 has been measured [*Rawlins et al.*, 1989] and a recent review [*Herron*, 1999] recommended an Arrhenius form for temperature dependence with an activation energy of 185 K throughout the thermosphere, i.e., has recommended a nearly temperature-independent rate coefficient.

[3] In this letter we report a first principles calculation of the rate coefficient for the reaction of $N(^2D)$ with O_2. Section 2 briefly describes the quasiclassical trajectory (QCT) calculation, integrating Hamilton's classical equations of motion on recently calculated $N(^2D)+O_2$ potential energy surfaces (PES) [*González et al.*, 2001a, 2001b, 2001c; *Braunstein and Duff*, 2000], used to obtain the reaction cross section as a function of collision energy. Since $N(^2D)$ atoms are produced in the thermosphere with excess translational energy the question of the fraction of these atoms reacting before thermalizing [*Dothe et al.*, 1997] is explored in section 3, and their contribution to the NO production is determined by calculating the Energy Distribution Function (EDF) for $N(^2D)$ atoms, using the energy dependent cross section described in section 2. The temperature dependence of the $N(^2D)+O_2$ thermal rate coefficient is also presented. Finally, the results are summarized and their impact on the recent observations of dramatically enhanced 5.3 μm emission from NO in the thermosphere due to solar storms as well as thermospheric models of NO are discussed in section 4.

2. Calculation of the $N(^2D)+O_2$ Reaction Cross Section

[4] The QCT calculation of the reaction cross section and rate coefficient has been used by the authors in a number of situations and has given useful results [*Duff et al.*, 1994; *Duff and Sharma*, 1996, 1997]. Four potential energy surfaces, 2 $^2A'$, 1 $^2A''$, 2 $^2A''$, 3 $^2A'$, contribute to the reaction cross-section and rate coefficient [*Braunstein and Duff*, 2000; *González et al.*, 2001a]; the first two making a
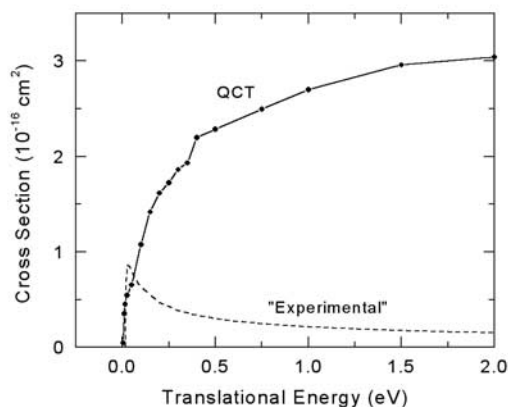
Figure 1. Calculated and "experimental" cross sections as a function of the initial relative translational energy. The experimental cross section is based on the dependence of the rate coefficient in the 200–600 K range.

Table 1. Sources and Sinks of N*(^{2}D) Atoms

Sources

$h\nu + N_2 \rightarrow N^*(^2D) + N^*(^4S)$

$h\nu + N_2 \rightarrow e + \frac{1}{2}N^*(^2D) + \frac{1}{2}N^*(^4S) + N^+$

$e + N_2^+ \rightarrow N^*(^2D) + N^*(^4S)$

$e + NO^+ \rightarrow N^*(^2D) + O$

$N_2^+ + O \rightarrow N^*(^2D) + NO^+$

$N^+ + O_2 \rightarrow N^*(^2D) + O_2^+$

Sinks

$N^*(^2D) + O \rightarrow N^*(^4S) + O$

$N^*(^2D) + O_2 \rightarrow NO(v,j) + O$

Translational Thermalization

$N^*(^2D) + M \rightarrow N(^2D) + M$ M = {N$_2$, O$_2$, O}

dominant contribution to the rate coefficient at the thermospheric temperatures, while the higher lying doublet and quartet states are less important due to the large energy barriers ($E_b \geq 0.35$ eV $\approx$ 4000 K) for reaction. QCT calculations are performed using the 1 ^{2}A$''$ and 2 ^{2}A$'$ adiabatic potential energy surfaces of *González et al.* [2001b, 2001c], and the 2 ^{2}A$''$, 3 ^{2}A$'$ surfaces of *Braunstein and Duff* [2000]. Thermal reaction rate coefficients and energy-dependent reaction cross sections are calculated using standard Monte-Carlo techniques [*Duff et al.*, 1994]. The reaction attributes from these surfaces are calculated independently and combined with the electronic degeneracy factor of ~1/15 for each state. A comparison of the population of the vibrational and rotational levels of nascent NO with the experimentally determined distribution is currently underway and will be given elsewhere. Figure 1 gives the reaction cross-section (σ_R) as a function of relative translational energy (E_T) using the QCT approach, and the estimated "experimental" cross section obtained from an inverse Laplace transform [*Sharma et al.*, 1998] of the recommended temperature dependence of the reaction rate coefficient [*Herron*, 1999]. Although the QCT cross-section shows no energy threshold, i.e., the reaction proceeds even at very small relative translational energies albeit slowly, the energy dependence of the reaction cross-section ($\sigma_R(E_T) \sim \sqrt{E_T}$) up to 0.4 eV relative translational energy suggests a different temperature dependence for the rate coefficient, $k(T) \sim T$, than previously given, $k(T) \sim e^{-185/T}$.

3. Thermalization and Reaction Rate of N(^{2}D) Atoms

[5] The contribution of nonthermal N(^{2}D) atoms to the reaction rate coefficient is taken into account by an integration of the QCT energy-dependent cross sections over the N(^{2}D) Energy Distribution Function (EDF). The EDF, which gives the fractional density of atoms with kinetic energy between E and E + dE (as measured in the laboratory frame), is obtained from the solution to the time dependent Boltzmann equation including source, sink and thermalization terms [*Dothe et al.*, 1997]. Processes leading to formation, destruction, and thermalization of translationally

hot N(^{2}D) atoms, denoted by N*(^{2}D), in the terrestrial thermosphere are given in Table 1. Rates of production of N(^{2}D) atoms are taken from Atmospheric Ultraviolet Radiance Integrated Code (AURIC) [*Strickland et al.*, 1999] for the geophysical parameters of 110 km altitude, 1400 hr local time, lat. 55N, lon. 169E, F10.7 = 170, and A$_p$ = 52. The corresponding source functions are shown as a function of kinetic energy in Figure 2. Sink functions are obtained in a similar manner, using a rate coefficient of 2×10^{-12} cm^3/s/molec for the quenching by O atoms, and the QCT energy-dependent cross sections for the reaction with O$_2$. The thermalizing terms are given by the QCT kernels of the N-N$_2$, N-O$_2$ and N-O interactions, as described in *Sharma et al.* [1998]. The time evolution of the EDF upon turning on the sources of Figure 2 at t = 0 s (initial N(^{2}D) density at t = 0 is zero), obtained by solving the time-dependent Boltzmann equation, is shown in Figure 3. The population after 1 s is nearly that at steady state and the steady-state EDF is nearly the same as the Maxwell-Boltzmann function at the local translational temperature, indicating a small contribution from nonthermal N(^{2}D) atoms. Figure 4 shows the steady-state and Maxwell-Boltzmann functions at 110 and 170 km altitude showing that the nonthermalized atoms make an even smaller contribution at the higher altitude. It was found that at 110 km altitude about 2% of the nonthermal N(^{2}D) atoms react before thermalization while at 170 km altitude this number is close to 0%.
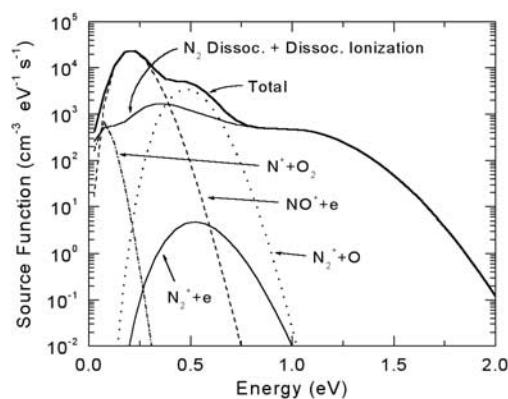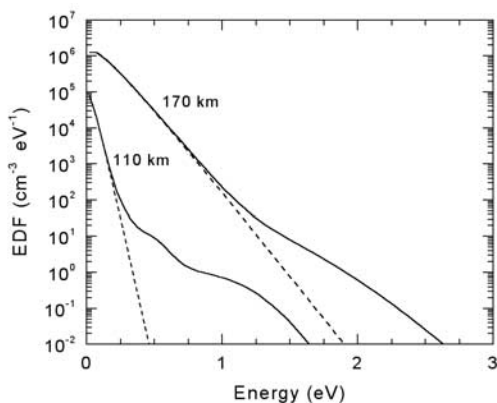

Figure 2. Energy dependence of the N(^{2}D) source functions as a function of energy at 110 km and local time 1400 hr, lat. 55N, lon. 169E, F10.7 = 170, and A$_p$ = 52.
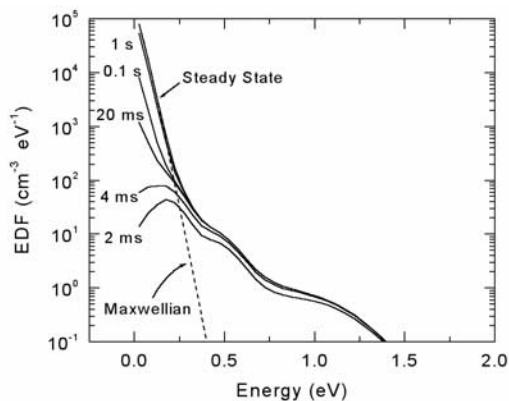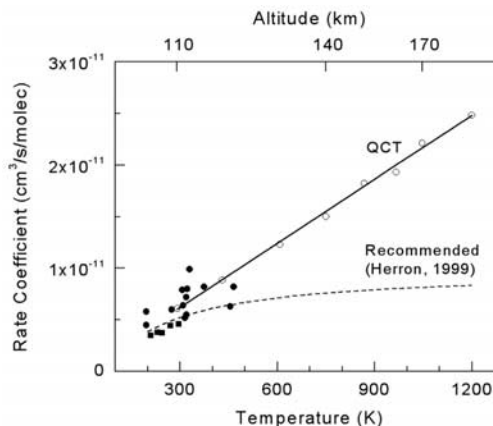
Figure 3. Time dependence of the N(^{2}D) energy distribution function as a function of energy at 110 km. Time after switching on the sources and sinks is shown as parameter. Curve labeled Maxwellian is the Maxwell-Boltzmann energy distribution function at the local translational temperature taken from AURIC.

Figure 5. Rate coefficient (cm^{3}s^{-1}molec^{-1}) as a function of temperature and altitude for the model atmosphere. The present calculation is labeled QCT. The temperature dependence of the rate coefficient recommended by *Herron* [1999] (dashed line), based on the data of *Jusinski et al.* [1988] (●) and *Shihira et al.* [1994] (■), is also shown.

[6] Figure 5 compares the calculated QCT rate coefficient of the N(^{2}D)+O$_2$ reaction as a function of temperature (and corresponding altitude for the model atmosphere) with the temperature-dependent measurements of *Jusinski et al.* [1988] and *Shihira et al.* [1994]. Also shown in this figure is the rate coefficient using the nearly temperature-independent expression recommended by *Herron* [1999]. The calculated rate coefficient, k(T) = 6.2 × 10^{-12} (T/300) cm^3/s/molec, provides a good representation of the measured temperature dependence in the temperature range of 195 K– 465 K, although there is scatter in the data. Nevertheless, there is significant disagreement between the temperature dependence of the present results and that recommended by *Herron* [1999]. In particular, although there is good agreement at low temperatures, the QCT rate coefficient is almost a factor of 4 greater than that obtained from the recommended form of the rate coefficient at 1200 K. This discrepancy suggests the importance of establishing the

temperature dependence of the N(^{2}D)+O$_2$ reaction in the laboratory.

4. Conclusions

[7] The new larger value of the rate coefficient for the production of NO given here impacts a number of issues connected with the modeling of the thermosphere:

1. *Dothe et al.* [2002a], using an auroral model [*Sharma et al.*, 2001] validated with data obtained at 110 km tangent altitude (temperature at the tangent altitude ≈300 K) by the Midcourse Space Experiment (MSX) satellite, modeled auroral data gathered at 195 km altitude (temperature at the tangent altitude ≈1000 K) by the space shuttle experiment Cryogenic Infrared Radiance Instrumentation for Shuttle (CIRRIS-1A) and found that modeled 5.3 μm emission from NO was a factor of three smaller than observed. The plausible hypothesis that the model gave a smaller emission because of the use of the previously recommended rate coefficient is currently being investigated.

2. The SABER (Sounding of the Atmosphere by Broadband Emission Radiometery) instrument aboard TIMED (Thermosphere, Ionosphere, Mesosphere, Energetics and Dynamics) satellite observed large increase (about twenty-fold around the poles) in the 5.3 μm emission at 110 km altitude following solar coronal mass ejection events on 20 April 2002 [*Russell et al.*, 2002]. This large increase can come about in two ways: (1) an increase in the total density of NO produced by the reaction with O$_2$ of N(^{2}D) atoms produced by the incoming particles, and (2) chemiluminescent emission from nascent highly vibrationally excited NO produced by this reaction. *Dothe et al.* [2002b] have pointed out that about 30% of the emission observed by SABER at low latitudes is due to the nascent NO. An increase in the rate coefficient of the N(^{2}D)+O$_2$ reaction at high altitudes is likely to have a large impact not only on the models of odd N but also on the models of the energy budget of the thermosphere as well.

Figure 4. Steady state (solid) and Maxwellian (dashed) energy distribution functions at 110 and 170 km altitude. Other geophysical parameters for the 170 km altitude calculation are the same as for the 110 km altitude calculation.

3. An increase in the rate coefficient of the N(^{2}D)+O$_2$ reaction at high altitudes is likely to have a large impact not only on the models of odd N but also on the models of the energy budget of the thermosphere as well. For example, the 5.3 μm cooling due to the impacts of atomic oxygen on NO varies linearly with NO density. This cooling process plays an important role in determining the temperature and density structure of the thermosphere [*Sharma and Roble*, 2001]. The large change in cooling thus produced suggests a reevaluation of the energy budget of the thermosphere. These issues will be fully investigated in future work.

References

Barth, C. A., Nitric oxide in the lower thermosphere, *Planet. Space Sci.*, *40*, 315–336, 1992.

Barth, C. A., S. M. Bailey, and S. C. Solomon, Solar-terrestrial coupling: Solar soft x-rays and thermospheric nitric oxide, *Geophys. Res. Lett.*, *26*, 1251–1254, 1999.

Braunstein, M., and J. W. Duff, Theoretical study of the N(^{2}D)+O$_2$(X$^3\Sigma_g^-$)→O+NO reaction, *J. Chem. Phys.*, *113*, 7406–7413, 2000.

Dothe, H., R. D. Sharma, and J. W. Duff, On the steady-state assumption for the energy distribution function of the nonthermal N(^{4}S) atoms and the efficiency of NO production by these atoms in the terrestrial thermosphere, *Geophys. Res. Lett.*, *24*, 3233–3236, 1997.

Dothe, H., J. W. Duff, R. D. Sharma, and N. B. Wheeler, A model of odd nitrogen in the aurorally dosed nighttime terrestrial thermosphere, *J. Geophysical Res.*, *107*(A6), 1071, doi:10.1029/2001JA000143, 2002a.

Dothe, H., J. W. Duff, R. D. Sharma, and J.-H. Yee, Sources of 5.3 μm emission from NO observed by SABER, *Eos Trans AGU*, *83*(47), Fall Meet. Suppl., SA72A-0516, 2002b.

Duff, J. W., and R. D. Sharma, Quasiclassical trajectory study of the N(^{4}S)+NO(^{2}Π)→N$_2$($^1\Sigma_g$)+O(^{3}P) reaction rate coefficient, *Geophys. Res. Lett.*, *23*, 2777–2780, 1996.

Duff, J. W., and R. D. Sharma, Quasiclassical trajectory study of the N(^{4}S)+NO(^{2}Π)→N$_2$($^1\Sigma_g$)+O(^{3}P) reaction cross section on the excited ^{3}A′ NNO surface, *Chem. Phys. Lett.*, *265*, 404–407, 1997.

Duff, J. W., F. Bien, and D. E. Paulsen, Classical dynamics of the N(^{4}S) + O$_2$→NO(X^{2}Π)+O(^{3}P) reaction, *Geophys. Res. Lett.*, *21*, 3043–3046, 1994.

González, M., I. Miquel, and R. Sayós, VTST kinetics study of the N(^{2}D)+O$_2$(X$^3\Sigma_g$)→NO(X^{2}Π) + O(^{3}P, ^{1}D) reactions based on CASSCF and CASPT2 ab initio calculations including excited potential energy surfaces, *Chem. Phys. Lett.*, *335*, 339–347, 2001a.

González, M., I. Miquel, and R. Sayós, *Ab initio*, variational transition state theory and quasiclassical trajectory study on the lowest ^{2}A′ potential energy surface involved in the N(^{2}D)+O$_2$(X$^3\Sigma_g^-$)→NO(X^{2}Π)+O(^{3}P) atmospheric reaction, *J. Chem. Phys.*, *115*, 2530–2539, 2001b.

González, M., I. Miquel, and R. Sayós, *Ab initio*, VTST, and QCT study of the 1 ^{2}A″ potential energy surface of the N(^{2}D)+O$_2$(X$^3\Sigma_g$)→NO(X^{2}Π)+O(^{3}P) reaction, *J. Chem. Phys.*, *115*, 8838–8851, 2001c.

Herron, J. T., Evaluated chemical kinetics data for reactions of N(^{2}D), N(^{2}P), and N$_2$(A$^3\Sigma_u^+$) in the gas phase, *J. Phys. Chem. Ref. Data*, *28*, 1453–1483, 1999.

Jusinski, L. E., G. Black, and T. G. Slanger, Resonance-enhanced multiphoton ionization measurements of N(^{2}D) quenching by O(^{3}P), *J. Phys. Chem.*, *92*, 5977–5982, 1988.

Rawlins, W. T., M. E. Fraser, and S. M. Miller, Rovibrational excitation of nitric oxide in the reaction of O$_2$ with metastable atomic atomic nitrogen, *J. Chem. Phys.*, *42*, 1097–1107, 1989.

Russell, J. M., et al., An Overview and Science Results from the SABER experiment on the TIMED Satellite, *Eos Trans AGU*, *83*(47), Fall Meet. Suppl., SA61A-01, 2002.

Sharma, R. D., and R. G. Roble, Impact of the new rate coefficients for the O atom vibrational deactivation and photodissociation of NO on the temperature and density structure of the terrestrial atmosphere, *J. Geophys. Res.*, *106*, 21,343–21,350, 2001.

Sharma, R. D., H. Dothe, and J. W. Duff, Model of the 5.3 μm radiance from NO during the day lit terrestrial thermosphere, *J. Geophys. Res.*, *103*, 14,753–14,768, 1998.

Sharma, R. D., R. O'Neil, H. Gardiner, J. Gibson, H. Dothe, J. W. Duff, P. P. Wintersteiner, and M. Kendra, MSX: Auroral enhancement of nitric oxide medium-wave infrared emission observed by the SPIRIT III radiometer, *J. Geophys. Res.*, *106*, 21,351–21,365, 2001.

Shihira, Y., T. Suzuki, S.-I. Unayama, H. Umemoto, and S. Tsunashima, Reactions of N(2 ^{2}D) and N(2 ^{2}P) with O$_2$, *J. Chem. Soc. Faraday Trans.*, *90*, 549–552, 1994.

Siskind, D. E., J. T. Bacmeister, M. E. Summers, and J. M. Russell III, Two-dimensional model calculations of nitric oxide transport in the middle atmosphere and comparison with Halogen Occultation Experiment data, *J. Geophys. Res.*, *102*, 3527–3546, 1997.

Solomon, S. C., C. A. Barth, and S. M. Bailey, Auroral production of nitric oxide measured by the SNOE satellite, *Geophys. Res. Lett.*, *26*, 1259–1262, 1999.

Strickland, D. J., J. Bishop, J. S. Evans, T. Majeed, P. M. Shen, R. J. Cox, R. Link, and R. E. Huffman, Atmospheric Ultraviolet Radiance Integrated Code (AURIC): theory, software architecture, inputs, and selected results, *J. Quant. Spectrosc. Radiat. Transfer*, *62*, 689–742, 1999.

————————————

H. Dothe and J. W. Duff, Spectral Sciences, Inc., 99 South Bedford Street, Burlington, MA 01803-5169, USA.

R. D. Sharma, Space Vehicles Directorate/VSSSE, Air Force Research Laboratory, Hanscom AFB, MA 01731-3010, USA. (Ramesh.Sharma@hanscom.af.mil)